Jurnal
Teknologi

Full Paper

NUMERICAL INVESTIGATION ON THE EFFECTS OF TBM FACE SUPPORT PRESSURES–A PARAMETRIC STUDY

Khoo Chee Min*

Department of Civil and Environmental Engineering, Universiti Teknologi PETRONAS, 32610 Seri Iskandar, Perak, Malaysia

Article history
Received
9 May 2024
Received in revised form
14 July 2024
Accepted
5 August 2024
Published Online
20 February 2025

*Corresponding author
chee_16005101@utp.edu.my

Graphical abstract

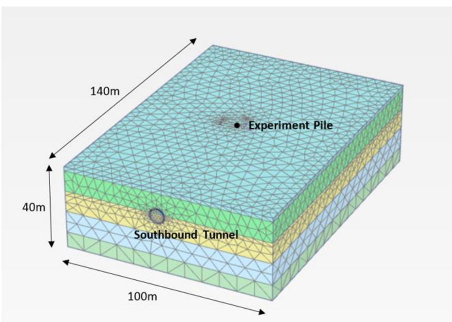

Abstract

Shield tunnelling operations, particularly those employing pressurized face tunnel boring machines (TBMs) such as earth pressure balance and slurry shields, are complex processes influenced by various driving parameters. Among these parameters, face support pressure plays a critical role in controlling ground and pile responses induced by tunnelling. This paper presents a numerical investigation on the effects of TBM face support pressures through a parametric study. Using data obtained from full-scale field research and through a validated numerical framework, this study aims to investigate how variations in TBM face support pressures affect pile responses and ground settlement during tunnelling operations. The findings emphasize the necessity of maintaining adequate face support pressures to mitigate excessive ground settlement and pile deformations. Notably, an optimum face support pressure range between 0.8 to 1.1 times the overburden pressure was identified, associated with minimal pile responses and ground settlement. These insights provide valuable guidance for optimizing face support pressure management strategies in shield tunnelling projects.

Keywords: Numerical simulation, parametric study, shield tunnelling, face support pressure, tunnelling-induced pile responses

Abstrak

Operasi pengorekan terowong berperisai, khususnya yang menggunakan mesin pengorekan terowong (*Tunnel Boring Machine*, TBM) bertekanan muka seperti *earth balance pressure* dan *slurry shields*, merupakan proses kompleks yang dipengaruhi oleh pelbagai parameter permanduan. Antara parameter-parameter ini, tekanan sokongan muka memainkan peranan penting dalam mengawal tindak balas tanah dan cerucuk akibat pengorekan terowong. Kertas kerja ini menyajikan penyiasatan berangka mengenai kesan tekanan sokongan muka TBM melalui satu kajian parameter. Dengan menggunakan data yang diperolehi daripada penyelidikan tapak berskala penuh dan melalui kerangka berangka yang disahkan, kajian in bertujuan untuk menyiasat bagaimana variasi tekanan sokongan muka TBM ini mempengaruhi tindak balas cerucuk dan pemendapan tanah semasa operasi pengorekan terowong. Penemuan kajian ini menekankan keperluan untuk mengekalkan tekanan sokongan muka yang mencukupi untuk mengurangkan pemendapan tanah yang berlebihan dan deformasi cerucuk. Julat tekanan sokongan muka antara 0.8 hingga 1.1 kali tekanan tanah adalah didapati optimum dalam pengawalan tindak balas cerucuk dan pemendapan tanah yang minima.

Kata kunci: Simulasi berangka, kajian parameter, pengorekan terowong berperisai, tekanan sokongan muka, tindak balas cerucuk akibat pengorekan

1.0 INTRODUCTION

1.1 Background

Shield tunnelling operations, particularly those employing pressurized face tunnel boring machines (TBMs) such as earth pressure balance (EPB) and slurry shields, are complex processes influenced by various parameters. Among these parameters, face support pressure plays a critical role in controlling ground and structure responses to tunnelling effects.

Recently, a full-scale field research was conducted at the tunnelling site of Malaysia's Klang Valley Mass Rapid Transit – Putrajaya Line project. The study utilized a combination of field measurements and numerical simulation to investigate tunnel-soil-pile interaction at differect stages of tunnel excavation. An extensively instrumented experiment pile, equipped with distributed fibre optical sensing technology, was installed, pre-loaded, and continuously monitod in real-time throughout the tunnel construction process. The measurement results were cross-validated through three-dimensional finite element modelling using recorded TBM driving data. The validated numerical framework has opened avenues for further exploration through numerical parametric studyies.

This paper presents a numerical evaluation of the impacts of TBM face support pressures on a loaded pile. It aims to investigate how variations in TBM face support pressures affect pile responses, ground surface settlement, and other related factors during tunnelling operations. The findings contribute to a deeper understanding of the mechanisms governing tunnelling-induced pile movements and provide insights for optimizing face support pressure management strategies in shield tunnelling projects.

1.2 The Research Study

The research site is situated at the Education Quarters along Jalan Raja Muda Abdul Aziz, Kampung Bharu, within the central business district of Kuala Lumpur. The 6.35 m diameter twin bored tunnels, constructed using closed face tunnel boring machine (TBM) and 275 mm thick pre-cast steel fibre reinforced concrete segmental linings, traverse through the Quarters, starting from the northwest at Hospital Kuala Lumpur Cross-over and extending southeastward to Raja Uda Station, as illustrated in Figure 1.

Variable density tunnel boring machines were selected for excavating the tunnels. This type of TBM can operate in four different tunnelling modes, making it adaptable to different geological conditions [1-4]. It is a further develpment of the multi-mode TBM, which combines the advantages of the EPB and slurry supported mix-shield modes [5]. Specifically, the TBMs were operated in EPB mode for this tunnelling section. Table 1 provides key technical data for the TBM, which featured a cutting diameter of 6,670 mm.

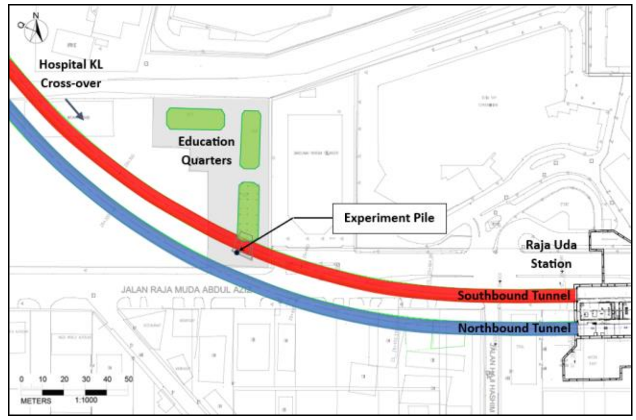

Figure 1 Location plan of the research site

Table 1 Key technical data of tunnel boring machine

Description	Data
Machine type	Variable Density TBM
Length TBM + back-up	ca. 135 m
Weight TBM + back-up	ca. 876 ton
Front shield diameter	6,620 mm
Front shield length	3,755 mm
Centre shield diameter	6,610 mm
Centre shield length	3,645 mm
Tail skin diameter	6,600 mm
Taik skin length	3,785 mm
Correction curve radius (min.)	150 m
Working pressure (at axis)	5 bar
Cutterhead power	1280 kW
Torque	4329 kNm

The experiment pile, with a diameter of 300 mm and positioned 1.5 m away form the extrados of the tunnel, is reinforced with API (American Petroleum Institute) pipe measuring 177.8 mm in outer diameter and 10.36 mm in wall thickness. Installed to a depth of 1.5 m into the limestone bedrock at 32.3 m below ground level, the micropile (grade G30) is designed with a capacity of 600 kN. Details regarding pile set-up and pre-loading can be found in reference [6].

The in-pile instrumentation, including conventional vibrating wire strain gauges and inclinometer, as well as innovative fibre optic distributed sensors, was meticulously designed and arranged to provide real-time data on the tunnelling-induced pile responses. For details of the field measurement results and findings, please refer to references [7,8].

1.3 Ground Characterization

The research site is situated within Kuala Lumpur Limestone formation, characterised by flat terrain with an average elevation of Reduced Level (RL) 34 m above the mean sea level. Site investigation confirmed the expected regional geological setting, revealing alluvium overlying limestone bedrock [9]. However, the presence of erractic bedrock levels, possibly containing cavities due to the inherent karstic nature of limestone formation, was anticipated. The alluvium consists mainly of interbedded layers of loose sand and soft clay/silt. Groundwater was encountered at a depth of 4 m at the site, with a typical seasonal fluctuation of ±0.5 m. Figure 2 illustrates the interpreted geological profile along the tunnel alignment, where the tunnel is located with cover-to-diameter ratios ranging from approximately 1.6 to 2.0.

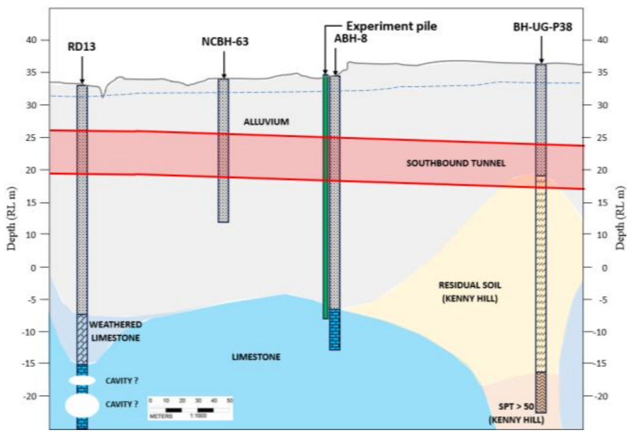

Figure 2 Interpreted geological profile

Figure 3 presents a plot of Standard Penetration Test (SPT) values versus depth for overburden soils, revealing consistently low SPT values in the surficial alluvium above the tunnel springline. To account for potential variations in soil properties, moderately conservative design lines are selected for the respective soil stratum.

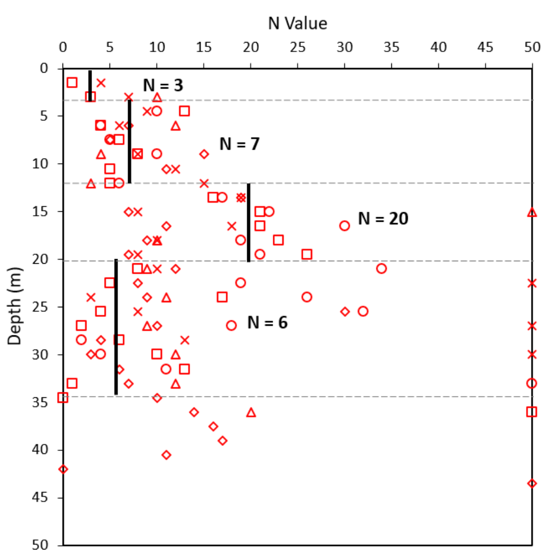

Figure 3 Design lines for geotechnical characteristics correlations

The modulus of elasticity (E_U) of the alluvial soils is obtained through cyclic pressuremeter tests and correlations with SPT values, as depicted in Figure 4.

The correlation factor for the alluvium suggests a relationship with E_U/SPT of 2N. For soils with lower SPT values (N < 10), a higher correlation factor of E_U = 2.5N is recommended for a more accurate interpretation. For detailed derivation of the other geotechnical parameters, please refer to reference [10].

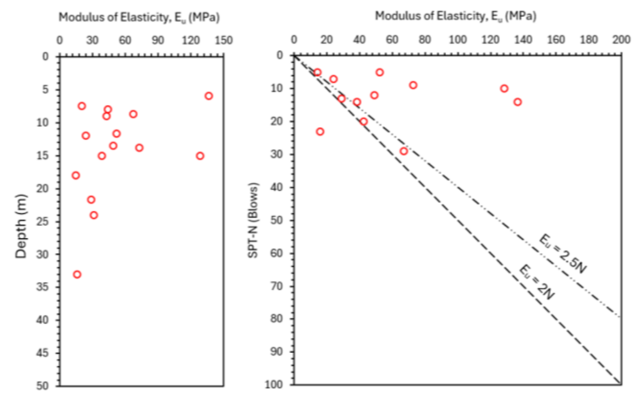

Figure 4 Modulus of elasticity and correlations with SPT values

2.0 METHODOLOGY

The parametric study was conducted through three-dimensional (3D) numerical modelling using a commercially available finite element program, PLAXIS 3D [11]. This software allowed for the simulation of tunnel advancement in a manner closely resembling the processes occurring during actual tunnel excavation. Generally, the accuracy of predictions made by a 3D model could be very good if a suitable constitutive soil model is employed, and the data functions, initial conditions, and boundary conditions are well controlled or known.

2.1 Model Set-up and Boundary Conditions

A full 3D model considering a height of 40 m and a width of 100 m has been adopted. The model's length is 140 m. These dimensions are considered sufficient to avoid any influence from the model boundaries. Lateral boundary fixity was assigned perpendicular to the vertical plane, while both lateral and vertical fixities were assigned to the bottom of the mesh. Consequently, movements normal to the vertical boundaries and in all directions of the base are restrained. The perspective view of the developed numerical model, consisting of 56,584 elements and 88,440 nodes, is presented in Figure 5. The model utilized a "medium" coarseness element distribution with 10-noded tetrahedral elements. The adequacy of the mesh density was assessed through iterative reruns with smaller mesh dimensions until displacement changes become insignificant [12,13], confirming that the current mesh is appropriate for the desiged level of accuracy.

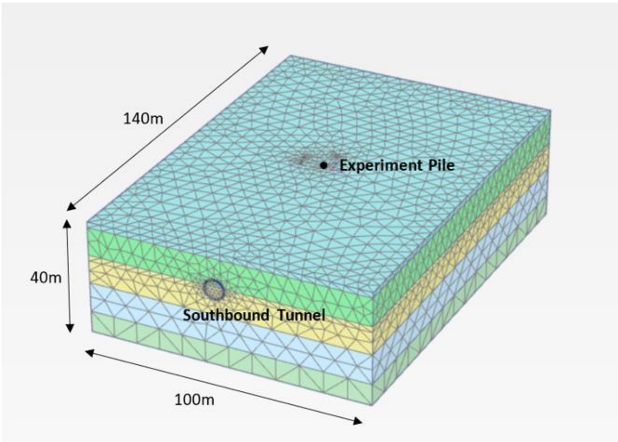

Figure 5 Perspective view of the developed 3D numerical model

The modelling approach involves the use of 10-node tetrahedral elements to represent the soils, structural components of the tunnel, and pile [14]. For the TBM and tunnel lining, curved plates in the form of shell elements are employed. The tunnel interface is modelled using the bi-linear Mohr-Coulomb model and is assigned to the tunnel extrados. The tunnel lining is assumed to be homogeneous and constructed at once. Additionally, tunnel circumferences are considered impermeable, allowing no drainage into the tunnel lining. The pile was modeled by using an embedded beam which consists of beam elements with embedded interface elements to describe the interaction with the soil at the pile skin and at the pile tip (bearing capacity).

2.2 Soil Constitutive Model and Material Properties

The Hardening Soil with Small Strain Stiffness (HS-Small) model [15], an extension of the Hardening Soil (HS) model, was utilized. This model introduces a formulation of small-strain stiffness properties in addition to the HS model, incorporating high initial elastic stiffness of soils denoted by the very small strain shear modulus (G_0). It also accounts for stiffness degradation with increasing strain in monotonic loading and stress path-dependent stiffness, including the regaining of high stiffness after sharp loading reversals [16]. The HS-Small model describes this behaviour using an additional strain-history parameter and two additional material parameters, G_0 and $\gamma_{0.7}$. The small strain threshold parameter ($\gamma_{0.7}$) represents the shear strain level at which the secant shear modulus (G_s) is reduced to approximately 70 % of G_0.

The geotechnical parameters, outlined in Table 2, were deduced from ground investigation data gathered at the tunnelling site. Oedometer loading/tangent stiffness (E_{oed}) was taken as E_{50}, and unloading/reloading stiffness (E_{ur}) was set as $3E_{50}$ by default in PLAXIS. The very small strain shear modulus (G_0) was empirically correlated with SPT values of 12N based on the work by Veeresh *et al.* [17].

The structural components of the tunnel, including the shield machine and lining, are represented as linear elastic materials in the model. Table 3 represents the properties assigned to these structural elements, especially the modelling of the TBM. The total weight of the TBM, excluding the back-up train, is defined as the weight per unit volume of the shield. The selection of Young's modulus and Poisson's ratio is determined by the material properties of the shield components. It is noteworthy that the interface is designed to be weaker and more flexible compared to the corresponding soil layer, reflected in a value less than 1.

Table 2 Geotechnical parameters of soils and rock

Parameter	Notation	Made Ground	Kenny Hill Residual Soil			Limestone
			N = 7	N = 20	N = 6	
Soil model	-	HS-Small	HS-Small	HS-Small	HS-Small	Mohr-Coulomb
Drainage type	Model	Drained	Drained	Drained	Drained	Drained
Unsaturated unit weight (kN/m^3)	γ_{unsat}	18.0	18.0	18.0	18.0	24.0
Saturated unit weight (kN/m^3)	γ_{sat}	19.0	19.0	19.0	19.0	24.0
Effective stiffness (kN/m^2)	E'_{ref}	-	-	-	-	1×10^6
Secant stiffness (kN/m^2)	E_{50}^{ref}	6×10^3	17×10^3	40×10^3	15×10^3	-
Tangent stiffness (kN/m^2)	E_{oed}^{ref}	6×10^3	17×10^3	40×10^3	15×10^3	-
Unloading/reloading stiffness (kN/m^2)	E_{ur}^{ref}	18×10^3	52×10^3	120×10^3	45×10^3	-
Poisson's ratio	ν	0.2	0.2	0.2	0.2	0.3
Power for stress-level dependency of stiffness	m	0.5	0.5	0.5	0.5	-
Shear modulus at very small strain (kN/m^2)	G_0^{ref}	36×10^3	84×10^3	240×10^3	72×10^3	-
Shear strain at $G_s = 0.722G_0$	$\gamma_{0.7}$	0.15×10^{-3}	0.15×10^{-3}	0.12×10^{-3}	0.15×10^{-3}	-
Cohesion (kN/m^2)	c'_{ref}	5	1	1	1	400
Friction angle (°)	ϕ'	28	30	32	30	32
Dilatancy angle (°)	φ	0	0	0	0	0

Table 3 Material properties – structural plate representing TBM

Parameter	Notation	Value
Material type	-	Elastic
Unit weight (kN/m³)	γ	247
Isotropic	-	Yes
Young's modulus (kN/m²)	E_{shield}	2.0 x 10⁹
Poisson's ratio	ν	0
Thickness (m)	d	0.17
Shear modulus (kN/m²)	G_{shield}	1.0 x 10⁹
Interface strength reduction	R_{inter}	0.9

Table 4 presents the properties of the tunnel lining used in the analysis. The elastic parameters, namely Young's modulus (E) and Poisson's ratio (ν), are derived from the material properties of steel fibre reinforced concrete (SFRC) lining. In the case of the lining, the interface strength reduction factor is set to one.

Table 4 Material properties – SFRC tunnel lining

Parameter	Notation	Value
Type of material behaviour	Model	Linear elastic
Material type	-	Non-porous
Volumetric weight (kN/m³)	γ_{unsat}	27.0
Young's modulus (kN/m²)	E_{ref}	3.1 x 10⁷
Poisson's ratio	ν	0.1
Interface strength reduction	R_{inter}	1.0

The experiment pile was modelled as an embedded beam with dimensions of 34 m in length and 300 mm in diameter. This model represented a cylindrical micropile (grade 30, API reinforcement). In the analysis, the effect of pile installation on pile behaviour and in-situ stress distribution of the soil was not considered. Therefore, a "wished-in-place" pile model was utilized, which closely resembles the behaviour of a bored pile or micropile. The interface between the soil and pile was simulated in the same way as that of the soil-tunnel lining interface. The material properites of the experiment pile are outlined in Table 5.

Table 5 Material properties – experiment pile

Parameter	Notation	Value
Type of material behaviour	Model	Elastic
Unit weight (kN/m³)	γ	6.0
Cross section type	-	Predefined
Predefined beam type	-	Solid circular beam
Diameter (m)	-	0.3
Young's modulus (kN/m²)	E_{ref}	1.2 x 10⁸
Axial skin resistance	-	Linear
Skin resistance at the top of the embedded beam (kN/m)	$T_{skin,start,max}$	200.0

2.3 Simulation Procedures of Tunnelling Process

In the finite element model, the first 42.8 m long of tunnels were modelled with "all-in-once installation" approach [18] and then followed by step-by-step simulation, with each excavation step corresponding to an advancement of the tunnel face by 1.4 m, which is equal to the width of a lining ring. The computation involves several construction steps in the shield tunnelling process:

(a) Excavation and Support Pressure Application: This step involves excavating the ground at the tunnel face while simultaneously applying the necessary support pressure to prevent active failure at the face.
(b) Tunnel Lining Installation: This step models the installation of the tunnel lining.
(c) Jacking Force Application: Applying the jacking force to propel the TBM forward.
(d) Grout Injection: Injecting grout behind the segments to fill the gap between the soil and the newly installed lining.

These construction steps are iteratively applied as the TBM advances, ensuring a comprehensive simulation of the advancing tunnel construction process. For further verification and validation of these simulation techniques, readers are encouraged to refer to the work carried out by Khoo *et al.* [19].

2.4 Variation of Face Support Pressures

The application of face support pressure is normalized to the overburden pressure (p_f/σ) at the tunnel crown level, with specified variations as outlined in Table 6. These diverse ranges are calibrated to the validated research site data to observe pile responses and the magnitude of ground surface settlement while maintaining consistent soil properties, pile properties, and other TBM driving parameters. The analyses aim to ascertain the relationship between applied face pressure and key effects on pile responses, including pile head displacement, pile lateral deflections (perpendicular and parallel to the tunnel), and pile axial load.

Table 6 Variation of face support pressure

Face Pressure, p_f (kN/m²)	Ratio to Baseline	p_f/σ
48.75	0.25	0.3
97.50	0.50	0.5
146.50	0.75	0.8
195.00	1.00	1.1
243.75	1.25	1.4
292.50	1.50	1.6
341.25	1.75	1.9
390.00	2.00	2.2

When the normalized face pressure (p_o/σ) exceeds 1.0, a negative face loss scenario occurs. Otherwise, it is considered as positive face loss, where the face pressure is within the range of overburden pressure or significantly lower than the overburden pressure.

For each applied face pressure, the evolution of the impacts is studied for a distance of TBM advance from y = -2D up to y = 9D from the experiment pile, where y is the distance between the TBM face and the experiment pile, normalized by the tunnel diameter (D). The negative distance signifies the TBM's position prior to reaching the pile. This range of distance is selected considering the recommended zone of influence from the research study [9] as well as a sufficiently long distance for stabilising the equilibrium of tunnelling effects.

3.0 RESULTS AND DISCUSSION

3.1 Model Calibration and Validation

The calibration and validation of the numerical model begins with comparisons between the computed results and the measured values for the pre-tunnelling conditions. Figure 6 presents the computed load-settlement behavior alongside a comparison with the measured changes in pile head settlements. At the 600 kN working load, the computed pile head settlement is 1.15 mm, compared to the field result of 1.18 mm. After the passage of the TBM at a sufficient distance, the pile was fully unloaded, resulting in a residual settlement of 0.16 mm, while the computed residual settlement is 0.18 mm. The remarkable agreement between computed and measured pile head settlements signifies the accuracy of the numerical simulation.

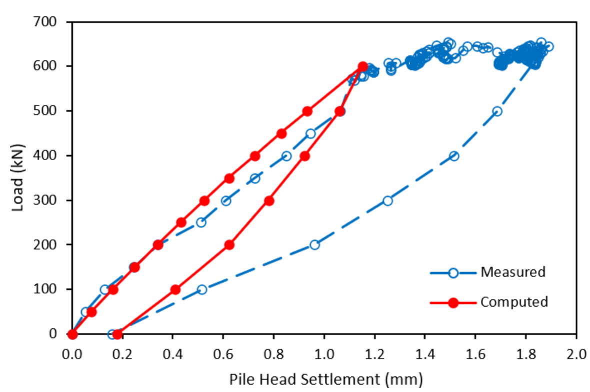

Figure 6 Load settlement behavior of the experiment pile

Additionally, Figure 7 illustrates the pile load distribution computed from the numerical simulation, juxtaposed with field measurement data from fibre optic sensors and vibrating wire strain gauges. Once again, there is excellent agreement between the analysis result and field measurements, confirming the successful validation of the numerical model and baseline parameters.

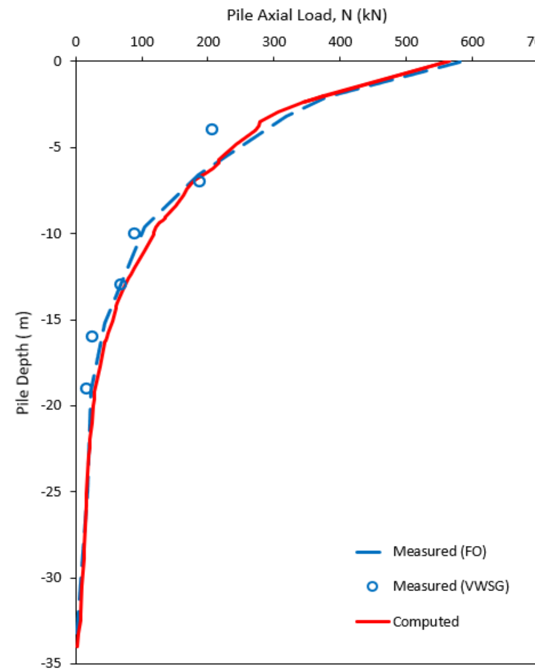

Figure 7 Axial load distribution along the experiment pile

3.2 Pile Head Displacement

Figure 8 illustrates the pile head settlement at various p_f/σ values. Generally, it can be observed that the pile head experiences a lesser magnitude of settlement within the range of p_f/σ between 0.8 and 1.1. This trend is evident as the TBM passes by the pile until a distance of y = 3D. However, there is a noticeable increase in pile head settlement when p_f/σ exceeds 1.1.

It should be emphasized, however, that the numerical model fails to converge if p_f/σ is less than 0.5. This implies that a minimum face support pressure is required for the successful simulation of this project case study. In practice, if the face support pressure decreases further, significant deformation or total collapse of the soil body may occur.

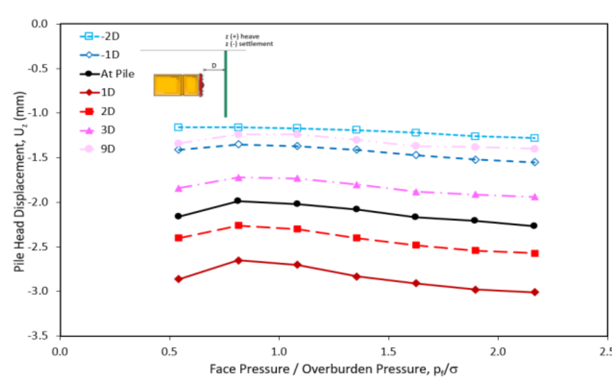

Figure 8 Pile head displacement, U_z vs. face pressure/overburden pressure, p_f/σ

3.3 Pile Lateral Deflections

Figure 9 illustrates the maximum pile lateral deflections at various p_f/s values for the transverse direction (perpendicular to the tunnel). Positive values indicate movement away from the tunnel extrados. Generally, the pile lateral deflection becomes noticeable in the transverse direction when the p_f/σ ratio is about 1.4 or higher. The same trend is observed for an approaching TBM at y = -1D, with the magnitude of deflection continuously increasing until the TBM has passed far beyond the pile.

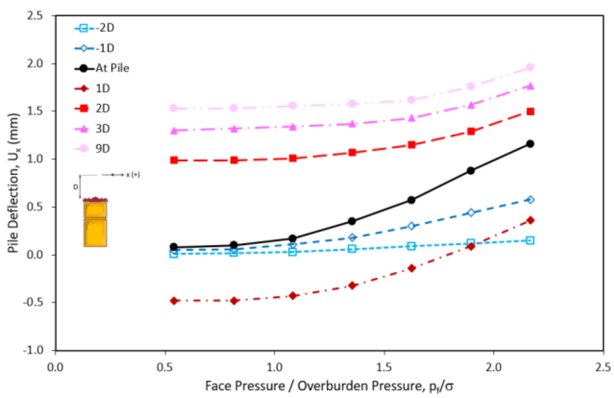

Figure 9 Pile lateral deflection, U_x vs. face pressure/overburden pressure, p_f/σ

The evolution of pile lateral deflection profiles is illustrated in Figure 10. From here, we can see that the pile movement path is obvious, especially for the case of negative face loss (p_f/σ > 1.0), where the pile is being pushed away when the TBM is approaching and being pulled inward at y = 1D (where the shield is passing through the pile) temporarily before release outward after the entire TBM shield has passed beyond the pile a distance of y = 2D. The maximum pile lateral deflection occurs in a zone above the tunnel springline to the tunnel crown.

Opposite to the transverse direction, the magnitude of pile lateral deflection in the longitudinal direction significantly and linearly increases with the increased p_f/σ ratio, even from a lower ratio of 0.5, as shown in Figure 11. Logically, a higher face pressure applied will directly push the pile forward along the tunnel alignment. The pile lateral deflection reaches its peak when the TBM face approaches the pile and starts to decrease after the TBM passed beyond.

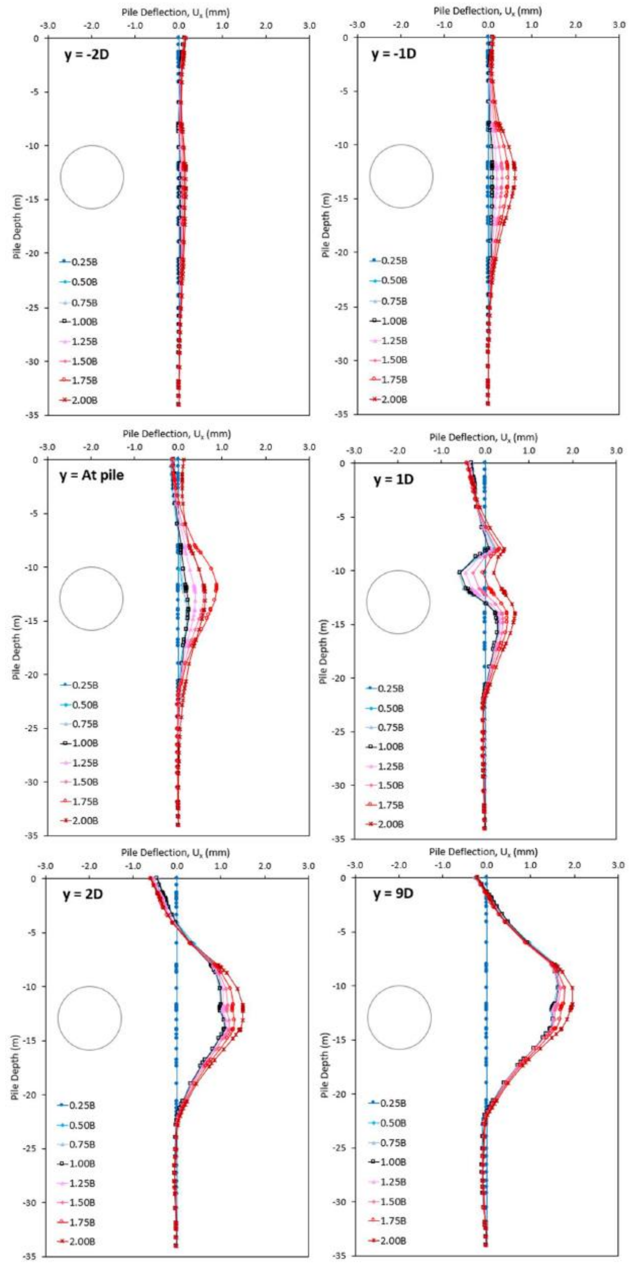

Figure 10 Evolution of pile lateral deflection, U_x profile

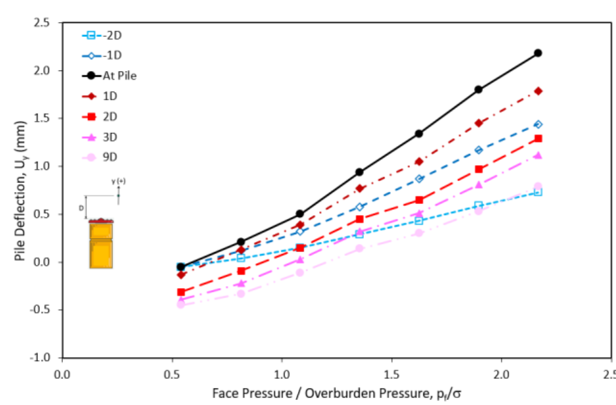

Figure 11 Pile lateral deflection, U_y vs. face pressure/overburden pressure, p_f/σ

In a similar presentation, Figure 12 illustrates the evolution of pile lateral deflection in the longitudinal direction. Similar pile movement behavior is noted except that the incurred inward movements are irreversible as observed when TBM passed far beyond the pile, y = 9D. This observation tallies with the hypothesis proposed by Loganathan [20] for a negative face loss tunnelling environment, where the ground is pushed away from the TBM face, may induce heave at the surface and subsurface ground movement away from the TBM face, subsequently, when the TBM has passed, a positive shield and tail loss occurs, signifying the closing of the physical gap. This results in the ground movement toward the tunnel, leading to ground settlement.

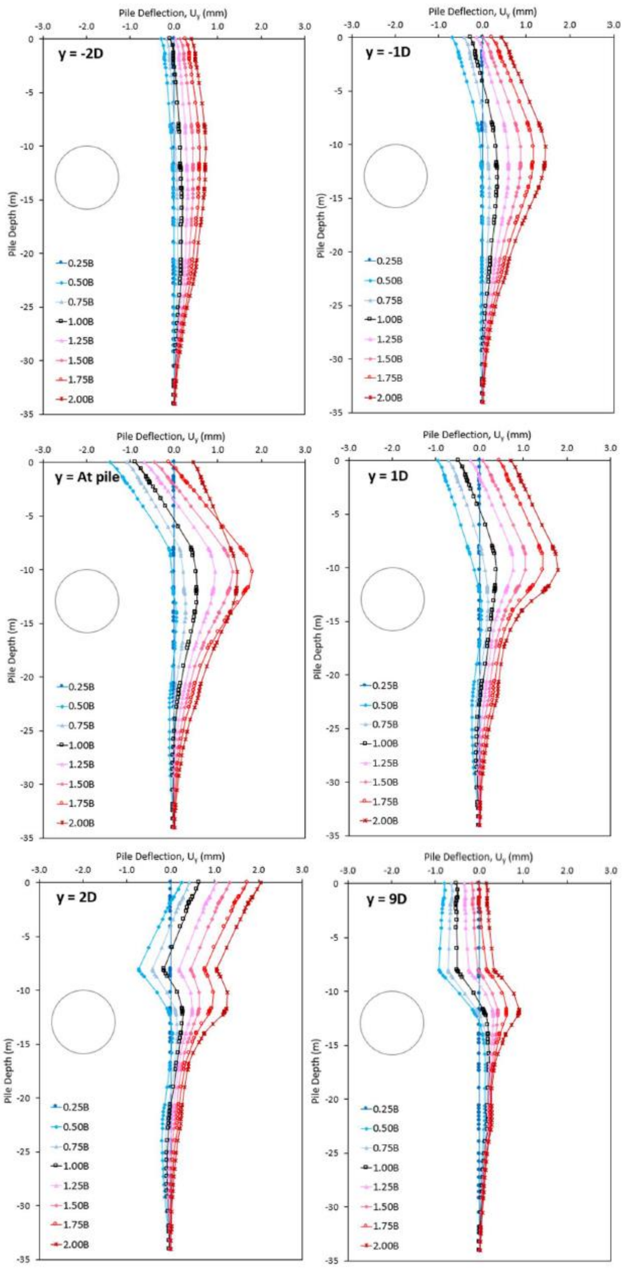

Figure 12 Evolution of pile lateral deflection profile, U_y

3.4 Pile Axial Load

Regarding the pile axial load, the evaluation focuses on the maximum value occurring in the critical zone between one time diameter above and below the tunnel horizon. This is crucial as the maximum axial load, attributed to the additional drag load due to tunnelling-induced ground settlement, typically occurs at the tunnel horizon.

Figure 13 illustrates the impacts on pile axial load in response to the varying applied face pressure. Despite the pile axial load generally being unresponsive to higher face pressure, a reduced load is obtained when the p_f/σ ratio is around 0.8 to 1.1 as observed when the TBM is at y = 1D, as shown in Figure 13.

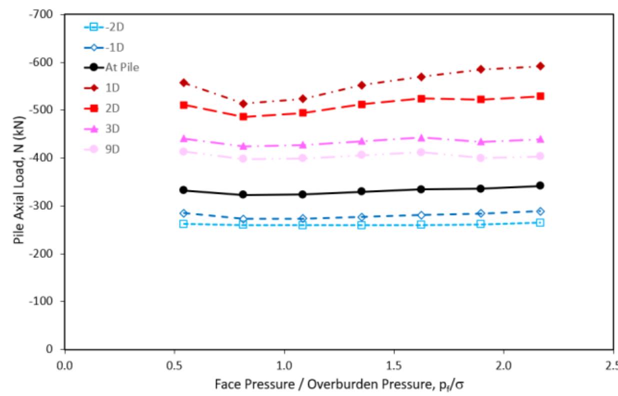

Figure 13 Pile axial load vs. face pressure/overburden pressure, p_f/σ

3.5 Ground Surface Settlement

Figure 14 illustrates the general trend of maximum ground settlement and ground loss obtained for the range of p_f/σ ratio adopted in this study. Clearly, the recommended optimum face pressure is between 0.8 to 1.1 times the overburden pressure, aligning with the earlier observations.

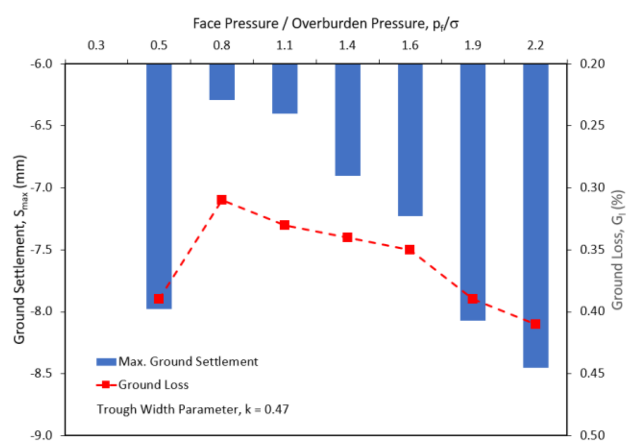

Figure 14 Ground settlement vs. face pressure/overburden pressure, p_f/s

4.0 CONCLUSION

This study conducted a comprehensive numerical investigation to analyse the effecs of varying face support pressures on tunnelling-induced pile responses and ground surface settlement, using data obtained from a full-scale field study. The calibration and validation of the numerical model against field measurements demonstrated the accuray and reliability of the simulation approach. The observed agreement (> 95%) between computed and measured pile head settlements, as well as pile load distributions, underscores the validity of the numerical framework established in this study.

The parametric analysis revealed clear distinctions, notably contrasting negative face loss, which occurs when normalized face pressure exceeds 1.0, with positive face loss observed when face pressure falls within the range of overburden pressure or significantly lower. This delineation sheds light on the critical role of face support pressure in influencing pile responses and ground behavior during tunnelling activities.

Significant patterns in pile displacements were observed, particularly regarding pile head settlement and lateral deflection, with notable variations observed across different stages of tunnel excavation. The investigation also extended to pile axial load, particularly in the critical zone around the tunnel horizon.

In summary, the findings emphasize the necessity of maintaining adequate face support pressures to mitigate excessive ground settlement and pile deformations. Notably, an optimum face support pressure range between 0.8 to 1.1 times the overburden pressure was identified, associated with minimal pile responses and ground settlement. These insights provide valuable guidance for optimizing face support pressure management strategies in shield tunnelling projects, ultimately enhancing the safety and stability of underground construction activities.

Acknowledgement

The author extends his gratitude to the management of Mass Rapid Transit Corporation Sdn Bhd for granting permission to publish this paper and for their positive support, which significantly contributed to the success of this work.

Conflicts of Interest

The author(s) declare(s) that there is no conflict of interest regarding the publication of this paper.

References

[1] Ooi, T. A. & Khoo, C. M. 2017. Tunnelling Activities in Malaysia – A Review. *Proceedings of Southeast Asian Conference and Exhibition on Tunnelling and Underground Space (SEACETUS 2017)*, Subang Jaya, Malaysia. 18–19 April 2017. 243–252.

[2] Klados, G., Ng, H. W., Wong, G. C. Y., and Chin, J. J. H. 2015. Managing Tunnelling Challenges through Kuala Lumpur Karst Formation using Variable Density TBMs. *Proceedings of International Conference and Exhibition on Tunnelling and Underground Space (ICETUS 2015)*, Kuala Lumpur, Malaysia. 3–5 March 2015. 186–191.

[3] Klados, G., Ng, H. W., and Hew, W. H. 2017. The Birth of a New Technology - The Variable Density Tunnel Boring Machine. *Proceedings of Southeast Asian Conference and Exhibition on Tunnelling and Underground Space (SEACETUS 2017)*, Subang Jaya, Malaysia. 18–19 April 2017. 59–62.

[4] Ooi, T. A. 2015. Tunnelling & Underground Space Development in Malaysia. Feature Article on variable Density TBM (VD-TBM) and Tunnelling and Underground Development in Malaysia. *IEM Bulletin*, February 2015.

[5] Schaub, W. & Duhme, R. 2014. Multi-mode and Variable Density TBMs Latest Trends in Developments. *Proceedings of Underground Singapore*.

[6] Khoo, C. M. 2024. The Transient Effects of Shield Tunnelling on a Loaded Pile. PhD Thesis. Universiti Teknologi PETRONAS.

[7] Khoo, C. M., Mohamad, H., Tee, B. P., and Ghazali, M. F. 2024. Field Measurement of Pile Transient Lateral Response to Advancing Tunnel. *Tunnelling for a Better Life* (ed. by Yan, J., Celestino, T., Thewes, M., and Eberhardt, E.). CRC Press, Taylor & Franics Group, London. 2672–2680.

[8] Khoo, C. M., Mohamad, H., Ghazali, M. F., Beddelee, A. A. A. M., Mohd Nasir, M. Y., and Thansirichaisree, P. 2025. Field Observation of Shield Tunnelling and Its Transient Effects on a Loaded Pile. *Geotechnical Engineering Journal of the SEAGS & AGSSEA*.

[9] Yin, E. H. 1976. Geological Map of Selangor, Sheet 94 (Kuala Lumpur). Geological Survey Department, Malaysia.

[10] Khoo, C. M., Mohamad, H., Beddelee, A. A. A. M., Thansirichaisree, P., Ghazali, M. F., and Mohd Nasir, M. Y. 2025. Transient Effects of Advancing Tunnel on a Loaded Pile: Numerical Analysis vs. Field Measurements. *Journal of Rock Mechanics and Geotechnical Engineering*.

[11] Brinkgreve, R. B. J., Kumarswany, S., and Swolfs, W. 2018. PLAXIS 3D Manual. PLAXIS B.V. The Netherlands.

[12] Khoo, C. M. 2024. Influence of 3-D Model Geometry on Numerical Simulation of Tunnelling Effects. *Proceedings of Southeast Asian Conference and Exhibition on Tunnelling and Underground Space (SEACETUS 2024)*, Kuala Lumpur, Malaysia. 5–7 March 2024. 195–200.

[13] Maleki, M. & Nabizadeh, A. 2021. Seismic Performance of Deep Excavation Restrained by Guardian Truss Structures System using Quasi-static Approach. *SN Applied Sciences*. 3: 262.

[14] Lee, S. W., Choy, C. K. M., Tse, S. C., van Gool, F. R., Cheang, W. W. L., and Brinkgreve, R. B. J. 2021. 3D Numerical Modelling of Tunnelling Intersecting Piles. Geotechnical Aspects of Underground Construction in Soft Ground (ed. by Viggiani). Taylor & Franics Group, London. 919–925.

[15] Schanz, T., Vermeer, P. A., and Bonnier, P. G. 2019. The Hardening Soil Model: Formulation and Verification. *Beyond 2000 in Computational Geotechnics*.

[16] Atkinson, J. H. 2000. Non-linear Soil Stiffness in Routine Design. 40th Rankine Lecture. *Géotechnique*. 50(5): 487–508.

[17] Veeresh, C., Goh, K. H., and Wen, D. 2015. Characterising the Small Strain Stiffness Behaviour of the Singapore Old Alluvium. *Proceedings of 15th Asian Regional Conference on Soil Mechanics and Geotechnical Engineering*. Fukuoka, Japan. 581–586.

[18] Vermeer, P. A., Bonnier, P. G., and Möller, S. C. 2002. On a Smart Use of 3D-FEM in Tunnelling.

[19] Khoo, C. M., Mohamad, H., Mohd Nasir, M. Y., and Thansirichaisree, P. 2024. Some Insights into Three-Dimensional Modelling of Tunnel Excavation. *International Journal of GEOMATE*. 27(120).

[20] Loganathan, N. 2016. Design Charts: Tunnelling-induced Effects on Adjacent Pile Foundation. *Proceedings of the 19th Southeast Asian Geotechnical Conference & 2nd AGSSEA Conference*. Kuala Lumpur, Malaysia. 1125–1130.